Microwave-assisted synthesis of nanocrystalline BaMoO$_4$ by a polymerized complex method and its photoluminescent property

JEONG HO RYU*†, BONG GEUN CHOI, SEON HYE KIM, JONG-WON YOON
Department of Ceramic Engineering, CPRC, Hanyang University, Seoul, 133-791, Korea
E-mail: jimihen@ihanyang.ac.kr

CHANG SUNG LIM
Department of Advanced Material Science and Engineering, CPRC, Hanseo University, Seosan, 356-706, Korea

KWANG BO SHIM
Department of Ceramic Engineering, CPRC, Hanyang University, Seoul, 133-791, Korea

BaMoO$_4$ is an important one among metal molybdate families that have a high-application potential in various fields, such as in photoluminescence [1] and hosts for lanthanide-activated lasers [2]. BaMoO$_4$ powders have usually been prepared by conventional methods consisting of repeated ball-milling and solid-state reaction of BaCO$_3$ and MoO$_3$ powders at high temperature [3]. However, BaMoO$_4$ powders prepared by the solid-state reaction are relatively coarse with inhomogeneous morphology and composition because the MoO$_3$ has a tendency to vaporize at high temperature [4].

These problems may be solved by applying an advanced wet chemical solution methods. Polymerized complex method as a modified Pechini method [5], where several metal ions in a solution could be first chelated to form metal complexes and then polymerized to form a gel, seems to be the most suitable among several chemical solution processes, because rigidly fixed cations are homogeneously dispersed in the polymer network and have few chances to segregate even during pyrolysis. This method has been used to successfully prepare highly pure samples of various oxides such as BaTiO$_3$ [6], Y$_6$WO$_{12}$ [7], and superconductors [8]. However, few studies on the chemical synthesis of BaMoO$_4$ by the polymeric complex method have been reported.

Microwave irradiation as a heating method has found and developed a number of applications in chemistry and ceramic processing [9–11]. Compared with the conventional methods, microwave synthesis has the advantages of very short reaction time, small particle size, narrow particle size distribution, and high purity. Jansen *et al.* [9] suggested that these advantages could be attributed to fast homogeneous nucleation and easy dissolution of the gel. In this work, the synthesis of homogeneous BaMoO$_4$ nanocrystalline powders using a modified polymerized complex method assisted by microwave irradiation is reported. Subsequently, the precursor and synthesized powders were evaluated for the crystallization process, particle morphology, and photoluminescent property.

Barium carbonate (BaCO$_3$) and ammonium molybdate ((NH$_4$)$_6$Mo$_7$O$_{24}$) were used as sources of the metallic cations. Ethylene glycol (HOCH$_2$CH$_2$OH, EG) and citric acid (HOC(CO$_2$H)(CH$_2$CO$_2$H)$_2$, CA) were used as solvent and chealating agent for the process. Fig. 1 shows the flow chart for the synthesis of nanocrystalline BaMoO$_4$ powders using a modified polymerized complex method assisted by microwave irradiation. The citrate solution was prepared by dissolving appropriate molar ratios of citric acid in ethylene glycol (CA:EG molar ratio = 1:4). After complete homogenization of the citrate solution, barium carbonate and ammonium molybdate were dissolved in the molar ratio of total chelate metal cations (TO) and citric acid (TO:CA molar ratio = 1:5). By keeping the solution at a temperature of 100 °C for 1 hr under constant stirring, the solution became viscous solution. A domestic microwave oven with 1200 W (Samsung Electronic Corp. Korea 2.45 GHz) was used for the reaction in the solution. The solution was placed in the microwave oven and the reaction was performed under ambient air for 30 min. The working cycle of the microwave oven was set between 40 s on and 20 s off. The solution became more viscous and the color changed to brown. No visible precipitation was observed during the heating process. As this solution condensed, the brown product was converted into powders after grinding with a Teflon bar. Thermal analysis was performed on this powder, hereinafter referred to as the "precursor". Heat-treatment of the precursor was performed at various temperatures from 300 to 500 °C for 3 hr in air.

The crystallization process was evaluated by thermogravimetry-differential thermal analysis (TG-DTA, SETRAM, France), using a sample weight of 10 mg and a heating rate of 5 °C/min. The existing phase in the particles after heat-treatment was identified by X-ray diffraction (XRD, CuK$_\alpha$, 40 kV, 30 mA,
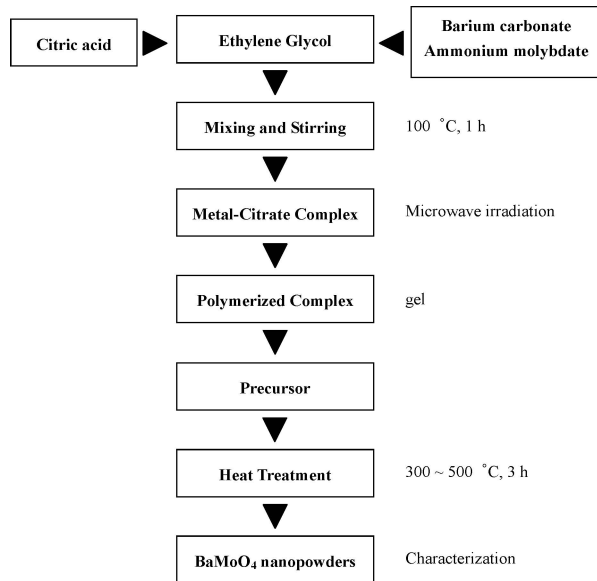
Figure 1 Flow chart for synthesis of nano-sized BaMoO$_4$ powders by the modified polymerized complex method using microwave irradiation.
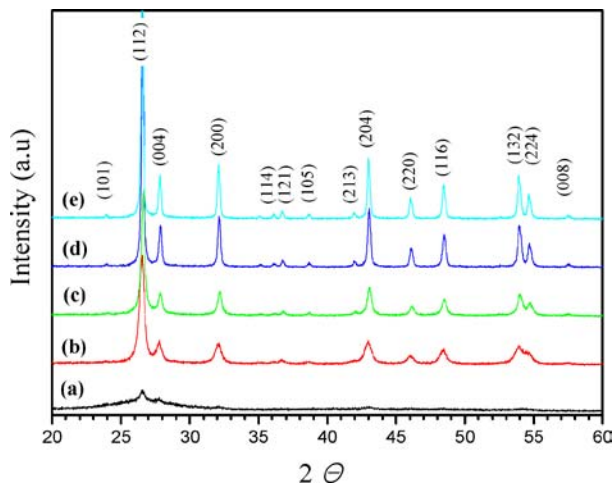

Figure 2 XRD patterns of the BaMoO$_4$ powders heat-treated at (a) 300, (b) 350, (c) 400, (d) 450, and (e) 500 °C for 3 hr.

Rigaku, Japan) with a scan rate of 3 °/min. The average crystalline size of the heat-treated powders was calculated using the XRD line broadening method through Scherrer's formula [12]. The microstructure and surface morphology of the powders were observed by transmission electron microscopy (TEM, JEM 2010, JEOL). The photoluminescent (PL) spectra were analyzed by a Japan Hitachi 850 Spectrophotometer.

The crystallization process of the precursor was evaluated by XRD, TG-DTA, and electronic diffraction pattern (EDP). Fig. 2 displays the phase identification of the BaMoO$_4$ powders heat-treated for 3 hr as a function of heating temperature in detail using XRD. In Fig. 2a, the powders of BaMoO$_4$ at 300 °C were amorphous with no crystallized phases. Above 350 °C in Fig. 2b–e, the powders were identified as BaMoO$_4$ phases, and un-reacted or additional phases were not detected.

Fig. 3 shows the TG-DTA curves for the BaMoO$_4$ precursor. In Fig. 3, with an increase of temperature, weight loss occurs in the TG curve up to 490 °C. There-
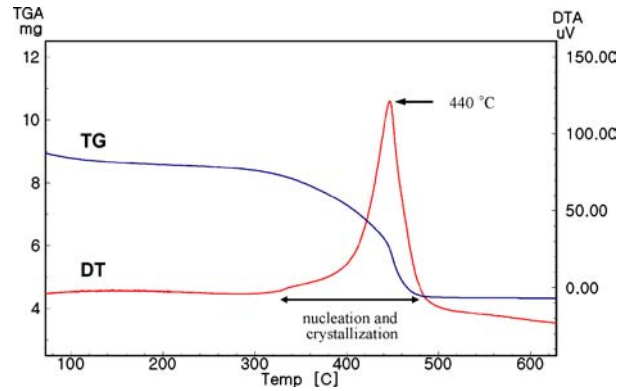

Figure 3 TG-DTA curves of the BaMoO$_4$ precursor in flowing air.

after the weight remains constant, indicating that the decomposition of all organic materials and crystallization of BaMoO$_4$ occurred below 490 °C. The DTA curve in Fig. 3 is interpreted as follows: (1) the increase of DT curve from 350 °C corresponds to initial decomposition of the precursor and formation of the nuclei of the nanocrystalline BaMoO$_4$; and (2) exothermic peak at 440 °C corresponds to the crystallization of BaMoO$_4$.

Fig. 4 shows TEM and electronic diffraction pattern (EDP) of the nanocrystalline BaMoO$_4$ powders prepared from 300 to 500 °C. The EDP of BaMoO$_4$ powders heat-treated at 300 °C in Fig. 4a showed only diffuse hollow rings, corresponding to an amorphous phase. With increasing temperature, at 350 °C in Fig. 4b, dotted rings were observed, signifying the nanocrystalline formation. The TEM morphology in Fig. 4b–d showed that the sizes of the crystallites gradually increased with the heating temperature. Most of the nanocrystalline powders of BaMoO$_4$ heat-treated between 400 and 500 °C showed primarily spherical morphology. The powders prepared at 500 °C have relatively spherical and a more homogeneous morphology with a narrow size distribution than those treated at the other temperatures.

The average grain sizes were determined from XRD powder pattern according to the Scherrer's equation [12]. $D = k\lambda/\beta\cos\theta$, Where D is the average grain size, k is a constant equal to 0.89, λ is the wavelength of X-rays equal to 0.1542 nm and β the corrected half-width that is obtained using (111) line of the pure silicon as the standard. Table I shows the average crystallite sizes for the heat-treated BaMoO$_4$ powders calculated by XRD line broadening method. The calculated average crystallite sizes of BaMoO$_4$ were 12, 17, 26, and 30 nm at temperatures of 350–500 °C. It is corresponding to the TEM in Fig. 4 indicating grain growth with increasing temperatures.

TABLE I Average crystallite size of BaMoO$_4$ crystallites as a function of heating temperature calculated by XRD line broadening method according to Scherrer's formula

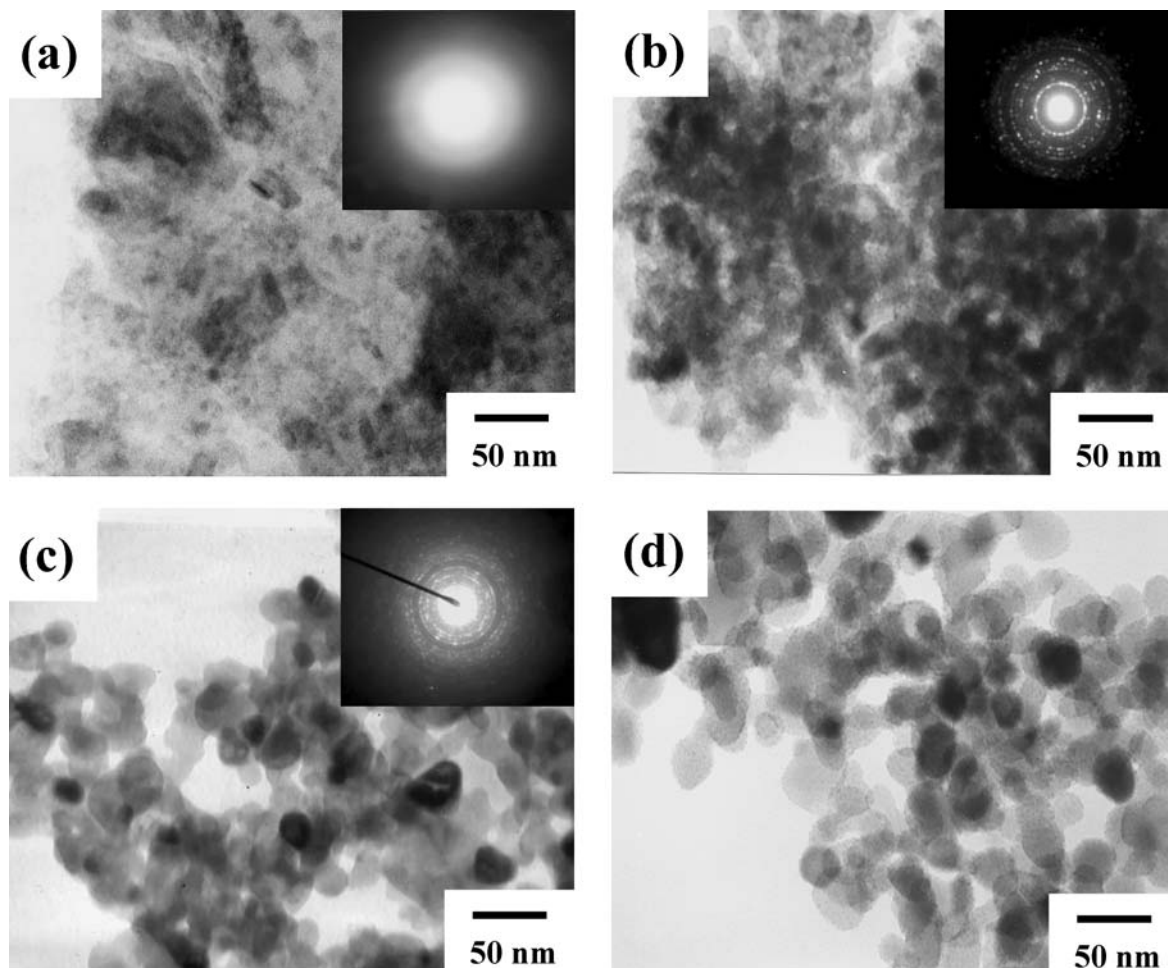| Temperature (°C)	Average crystallite size (nm)
350	12
400	17
450	26
500	30

Figure 4 TEM and EDP of nano-sized BaMoO₄ powders heat-treated at (a) 300, (b) 350, (c) 400, and (d) 500 °C for 3 hr.
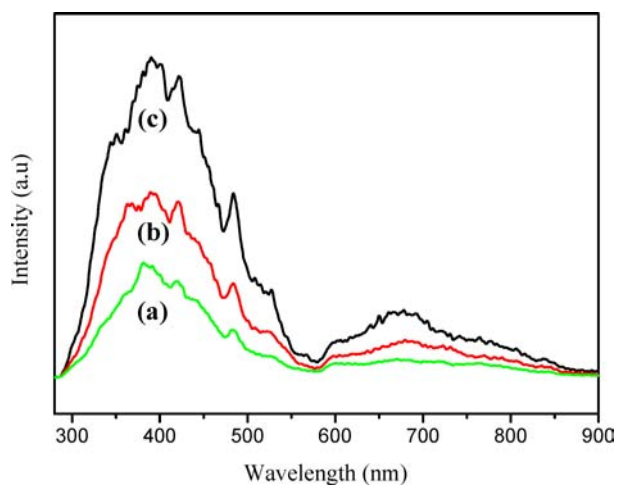

Figure 5 Emission spectra of the BaMoO₄ powders heat-treated at (a) 350, (b) 400, and (c) 500 °C for 3 hr.

Room-temperature photoluminescence (PL) of the prepared nano-sized BaMoO₄ powders are shown in Fig. 5. The PL of BaMoO₄ has been discussed in the frame of molecular orbital models of the $[\text{MoO}_4^{2-}]$ radicals [13]. It is generally assumed that the measured emission spectra of BaMoO₄ are mainly attributed to the charge-transfer transitions within the $[\text{MoO}_4^{2-}]$ complex [13]. With the excited wavelength at 240 nm, the powders exhibited blue emission near 400 nm in Fig. 5. Weak red emission bands near 670 nm were observed at longer wavelength and the additional emission

band can be ascribed to a defects structure [14]. The intensity of PL emission in nanocrystalline BaMoO₄ powders prepared at 500 °C is stronger than those of other temperatures, which indicates the great dependence of the PL properties on the morphology, crystallinity, and homogeneity of the BaMoO₄ powders. Generally, it is noted that particles with the shape of a non-agglomerate as well as high crystallinity plays an important role in the improvement of luminescent efficiency [15]. For the similar morphological samples, the homogenized particles must be favorable to PL characteristics because of less contamination or fewer dead layers on the phosphor surface [16]. Therefore, the enhancement of the PL intensity at 500 °C in Fig. 5 is attributed to the higher crystallinity, higher uniformity in particle size and more homogeneous particle morphology, which are corresponding to the analysis on XRD data and TEM morphology.

References

1. F. A. KROGER, in "Some Aspect of the Luminescence of Solids" (Elsevier, Amsterdam, 1948) p. 107.
2. A. M. LEJUS and R. COLLONGUES, in "Current Topics in Materials Science", edited by E. Kaldis (North-Holland Publishing Co., Amsterdam, 1980) p. 481.
3. C. PUPP, R. YAMDAGNI and R. F. PORTER, *J. Inorg. Nucl. Chem.* **31** (1969) 2021.
4. W. S. CHO, M. YASHIMA, M. KAKIHANA, A. KUDO, T. SAKATA and M. YOSHIMURA, *J. Am. Ceram. Soc.* **80**(3) (1997) 765.
5. M. P. PECHINI, U.S. Pat. No. 3330697, July 11, 1967.

6. S. KUMAR, G. L. MESSING and W. B. WHITE, *J. Am. Ceram. Soc.* **76** (1993) 617.
7. M. YOSHIMURA, J. MA and M. KAKIHANA, *J. Am. Ceram. Soc.* **81** (1998) 2721.
8. M. KAKIHARA, M. YOSHIMURA, H. MAZAKI, H. YASUOKA and L. BORJESSON, *J. Appl. Phys.* **71** (1992) 3904.
9. C. JANSEN, A. ARAFAT, A. K. BARAKAT, H. VAN BEKKUM, in "Synthesis of Microporous Materials Materials" (Van Nostrand Reinhold, New York, 1992) p. 507.
10. T. OHGUSHI and K. ISHIMARU, *J. Am. Ceram. Soc.* **84**(2) (2001) 321.
11. R. ROY, S. KOMARNENI and J. L. YANG, *J. Am. Ceram. Soc.* **68** (1985) 392.
12. B. D. CULLITY, in "Elements of X-ray diffraction" 2nd ed. (Addison-Wesley publishing company Inc., MA, 1978) p. 101.
13. D. A. SPASSKY, S. N. IVANOV, V. N. KOLOBANOV, V. V. MIKHAILIN, V. N. ZEMSKOV, B. I. ZADNE-PROVSKI and L. I. POTKIN, *Radiation Measurements* **38** (2004) 607.
14. R. GRASSER and A. SCHARMANN, *J. Luminescence* **12/13** (1976) 473.
15. G. Y. HONG, B. S. JEON, Y. K. YOO and J. S. YOO, *J. Electrochem. Soc.* **148**(11) (2001) H 161.
16. Y. C. KANG, H. S. ROH, E. J. KIM and H. D. PARK, *J. Electrochem. Soc.* **150**(4) (2003) H 93.